PHYSICAL REVIEW D **71,** 014502 (2005)

Penguin diagrams for improved staggered fermions

Weonjong Lee*

School of Physics, Seoul National University, Seoul, 151-747, South Korea

(Received 24 September 2004; published 19 January 2005)

We calculate, at the one-loop level, penguin diagrams for improved staggered fermion operators constructed using various fat links. The main result is that diagonal mixing coefficients with penguin operators are identical between the unimproved operators and the improved operators using such fat links as Fat7, Fat7 + Lepage, $\overline{\text{Fat7}}$, HYP (I) and HYP (II). In addition, it turns out that the off-diagonal mixing vanishes for those constructed using fat links of Fat7, $\overline{\text{Fat7}}$ and HYP (II). This is a consequence of the fact that the improvement by various fat links changes only the mixing with higher dimension operators and off-diagonal operators. The results of this paper, combined with those for current-current diagrams, provide complete matching at the one-loop level with all corrections of $\mathcal{O}(g^2)$ included.

DOI: 10.1103/PhysRevD.71.014502 PACS numbers: 11.15.Ha, 12.38.Gc, 12.38.Aw

I. INTRODUCTION

Decoupling of heavy particles in the standard model leads to the low-energy effective Hamiltonian through OPE (operator product expansion) which achieves a factorization of short- and long-distance contributions. The effective Hamiltonian of our interest consists of $\Delta S = 1$ four-fermion operators which contain information at low-energy and the corresponding Wilson coefficients including the short-distance physics at high energy. The low-energy effects of the electroweak and strong interactions can be expressed as matrix elements of the four-fermion operators between hadron states. Since the matrix elements involve nonperturbative QCD physics at low-energy, lattice QCD is well suited for their calculation. The main advantage of using lattice QCD is that it provide a first principle, nonperturbative estimate. Different fermion discretizations such as Wilson, staggered, domain-wall and overlap have been used to study the matrix elements and to control their statistical and systematic errors.

In this work, we adopt staggered fermions to explore the renormalization property of the operators relevant to calculating the weak matrix elements. Staggered fermions are an attractive choice for the calculation of weak matrix elements. They are computationally efficient and so simulations with three dynamical flavors are already possible with relatively light quark masses using the AsqTad staggered fermions [1]. They preserve enough chiral symmetry to protect operators of physical interest from mixing with others of wrong chirality. By construction they retain four tastes of doublers for each lattice field, which in itself is not a problem. Their main drawback is that the tastes symmetry is broken at nonzero lattice spacing and is restored in the continuum limit. At nonzero lattice spacing, quark-gluon interactions violate the taste symmetry. This has two consequences: first, there are large $\mathcal{O}(a^2)$ discretization errors in hadron spectrum and weak matrix elements and second, some one-loop corrections are so large that matching factors differ significantly from their tree-level value of unity.

Both problems are manifestly alleviated by improving staggered fermions using ''fat'' links [2,3]. Taste symmetry violations in the pion multiplet are substantially reduced [4,5] and one-loop corrections to the matching factors for four-fermion operators are reduced from as large as 100% down to $\sim$10% [6]. Based upon the analysis of Refs. [7,8], we figured out that the perturbative corrections is smallest for a particular type of fattening, ''HYP'' and ''$\overline{\text{Fat7}}$'' smeared links. Hence, we choose the ''HYP/$\overline{\text{Fat7}}$'' improvement scheme for our numerical study on the weak matrix elements [9].

Recently, there have been elaborate efforts to do the higher loop calculation for highly improved staggered fermions using the Luscher and Weisz method [10]. They automated the generation of the Feynman rules for essentially arbitrary complicated lattice actions such as the AsqTad type [11] and some even developed an algorithm which generates Feynman diagrams automatically [12].

An essential step for using lattice QCD is to obtain the relationship between the continuum and lattice four-fermion operators. There are two classes of Feynman diagrams at the one-loop level: (1) current-current diagrams and (2) penguin diagrams [13,14]. At the one-loop level, the contribution from the current-current diagrams and the penguin diagrams can be treated separately. In the case of the current-current diagrams, the matching coefficients for the operators constructed using improved staggered fermions (HYP/$\overline{\text{Fat7}}$) were presented in [6].

Here, we focus on penguin diagrams in which one of the quarks in the four-fermion operator is contracted with one of the antiquarks to form a closed loop. The main goal of this paper is to calculate the penguin diagrams for improved staggered fermion operators constructed using various fat links and to present the matching formula between the continuum and lattice operators at the one-loop level. The results are compared with those for the unimproved

*Electronic address: wlee@phya.snu.ac.kr

staggered fermions given in [14]. The role of improvement is reviewed from the standpoint of operator mixing. The main results of this paper, combined with those of current-current diagrams given in Ref. [6], provide a complete set of matching formula for ϵ'/ϵ at the one-loop level with all the g^2 corrections included.

This paper is organized as follows. In Sec. II, we describe our notation for the improved staggered fermion operators and various fat links. We also explain the Feynman rules. In Sec. III, we explicitly calculate penguin diagrams step by step and the main results are summarized in a theorem. We close with some conclusions in Sec. IV.

A preliminary result of this paper appeared in [15].

II. NOTATION AND FEYNMAN RULES

Basically, the improved staggered fermion action has the same form as for the unimproved staggered fermions [16], except in that the original thin links U_μ are replaced by fat links V_μ.

$$S = a^4 \sum_n \Big[\frac{1}{2a} \sum_\mu \eta_\mu(n) (\bar\chi(n) V_\mu(n) \chi(n+\hat\mu) - \bar\chi(n+\hat\mu) V_\mu^\dagger(n) \chi(n)) + m \bar\chi(n)\chi(n) \Big], \tag{1}$$

where $n = (n_1, n_2, n_3, n_4)$ is the lattice coordinate and $\eta_\mu(n) = (-1)^{n_1+\cdots+n_{\mu-1}}$. Here, the fat link V_μ represents collectively Fat7 [17], Fat7 + Lepage [18], HYP links [5] and SU(3) projected Fat7 ($\overline{\text{Fat7}}$) links [8]. The detailed definitions of various fat links are given in the original references and so we do not repeat them here. In addition, MILC and HPQCD Collaboration developed and have used the AsqTad staggered action [2–4,17], whose gauge action is a one-loop Symanzik improved action and whose fermion action contains a Naik term in order to remove the $O(a^2)$ discretization errors. Out of various choices, HYP and $\overline{\text{Fat7}}$ suppress, in particular, the taste-changing gluon interactions efficiently and reduce the taste symmetry breaking in the pion spectrum significantly [5], compared with others. In addition, it turns out that the one-loop corrections are smallest for HYP and $\overline{\text{Fat7}}$ compared with others [7] and that they possess several nice properties in renormalization which are explained in [8]. If the goal of the improvement were to minimize the $\mathcal{O}(a^2)$ discretization error and to achieve a better scaling behavior through the Symanzik improvement program, it would be natural to choose the action of the AsqTad type and improve the operators correspondingly. However, our improvement goal is to minimize the perturbative correction as much as possible (if possible, down to less than 10% at the one-loop level), which, in fact, turned out to be the same as to minimize the taste symmetry breaking effect [19]. Hence, we have chosen HYP/$\overline{\text{Fat7}}$ improvement scheme for our numerical study on ϵ'/ϵ mainly because it serves better to our purpose of improvement. In this paper, we adopt the same notation for fat links as in [6–8].

In order to construct the four spin component Dirac field, we adopt the coordinate space method suggested in [20]. In this method, we interpret 16 staggered fermion fields (χ) of each hypercube as four Dirac spin and four flavor (= taste) components. The continuum limit of the staggered fermion action on the lattice corresponds to QCD with four degenerate flavors ($N_f = 4$) [16]. There are numerous choices to transcribe the lattice operator for a given continuum operator [21–23]. We adopt the same convention and notation as in [24] except for the gauge links. We denote the gauge-invariant bilinear operators as

$$[S \times F] \equiv \frac{1}{N_f} \sum_{A,B} [\bar\chi_a(y_A) (\overline{\gamma_S \otimes \xi_F})_{AB} \chi_b(y_B)] \mathcal{V}^{ab}(y_A, y_B), \tag{2}$$

where S and F represent spin and flavor (= taste), respectively, and correspond to one of the following; S (scalar), V_μ (vector), $T_{\mu\nu}$ (tensor), A_μ (axial), and P (pseudoscalar). Here, $\mathcal{V}(y_A, y_B)$ is a product of gauge links that makes the bilinear operator gauge invariant. The link matrices $\mathcal{V}(y_A, y_B)$ are constructed by averaging over all of the shortest paths between y_A and y_B, such that the operator $[\gamma_S \times \xi_F]$ is as symmetric as possible:

$$\mathcal{V}(y_A, y_B) = \frac{1}{4!} \sum_P V(y_A, y_A + \Delta_{P1}) \cdots V(y_A + \Delta_{P1} + \Delta_{P2} + \Delta_{P3}, y_B), \tag{3}$$

where P is an element of the permutation group (1234) and

$$\Delta_\mu = (B_\mu - A_\mu)\hat\mu. \tag{4}$$

For the four-fermion operators, we use the same notation as the bilinears but need to distinguish between color one trace and color two trace operators.

$$[S \times F][S' \times F']_I \equiv \frac{1}{N_f^2} \sum_{A,B,C,D} [\bar\chi(y_A)(\overline{\gamma_S \otimes \xi_F})_{AB} \chi(y_B)] \cdot [\bar\chi(y_C)(\overline{\gamma_{S'} \otimes \xi_{F'}})_{CD} \chi(y_D)] \cdot \mathcal{V}(y_A, y_D) \mathcal{V}(y_C, y_B), \tag{5}$$

$$[S \times F][S' \times F']_{II} \equiv \frac{1}{N_f^2} \sum_{A,B,C,D} [\bar\chi(y_A)(\overline{\gamma_S \otimes \xi_F})_{AB} \chi(y_B)] \cdot [\bar\chi(y_C)(\overline{\gamma_{S'} \otimes \xi_{F'}})_{CD} \chi(y_D)] \cdot \mathcal{V}(y_A, y_B) \mathcal{V}(y_C, y_D). \tag{6}$$

Here, note that the subindices I, II represent the color one trace and color two trace operators, respectively. There are two completely independent methods to construct operators on the lattice using a Fierz transformation: one spin trace formalism and two spin trace formalism [21]. In this paper, we choose two spin trace formalism to construct the

lattice operators and it is also adopted for our numerical study on ϵ'/ϵ.

The Feynman rules for the unimproved staggered fermions are standard and presented in [14,21,24–28]. Here, we use the same notation for Feynman rules as in [21,24] and we do not repeat them. By introducing fat links, we need to change the Feynman rules. These changes in the Feynman rules originating from fat links are given in [6,7]. Here we adopt the same notation and Feynman rules as in [6,7]. We explain only the essential ingredients for a one-loop calculation.

We define the gauge fields of the thin link and fat links as

$$U_\mu(x) = \exp\left[iaA_\mu\left(x + \frac{1}{2}\hat{\mu}\right)\right], \tag{7}$$

$$V_\mu(x) = \exp\left[iaB_\mu\left(x + \frac{1}{2}\hat{\mu}\right)\right]. \tag{8}$$

Here, note that V_μ corresponds to various fat links. We call B_μ a "fat gauge field" and A_μ a "thin gauge field." This fat gauge field can be expressed in terms of thin gauge fields as follows:

$$B_\mu = \sum_{n=1}^{\infty} B_\mu^{(n)} = B_\mu^{(1)} + B_\mu^{(2)} + \mathcal{O}(A^3).$$

Here, $B_\mu^{(n)}$ represents a term of order A^n. Theorems 1 and 2 of [8] say that the linear term is invariant under SU(3) projection and that since the quadratic term is antisymmetric in thin gauge fields, its contribution vanishes at the one-loop level [29]. Hence, at one-loop level, the renormalization of the gauge-invariant staggered composite operators constructed using fat links of HYP type can be done by simply replacing the propagator of A_μ by that of $B_\mu^{(1)}$. This simplicity is extensively used to calculate the one-loop correction to the improved staggered operators [6,7].

The linear term $B^{(1)}$ can be expressed in momentum space as

$$B_\mu^{(1)}(k) = \sum_\nu h_{\mu\nu}(k) A_\nu(k).$$

The details of the blocking transformation for the fat links are contained in $h_{\mu\nu}(k)$, which is given in [6,7] for various fat links.

$$\begin{aligned} h_{\mu\nu}(k) &= \delta_{\mu\nu} D_\mu(k) + (1-\delta_{\mu\nu}) G_{\mu\nu}(k), \\ D_\mu(k) &= 1 - d_1 \sum_{\nu\neq\mu} \bar{s}_\nu^2 + d_2 \sum_{\substack{\nu<\rho \\ \nu,\rho\neq\mu}} \bar{s}_\nu^2 \bar{s}_\rho^2 - d_3 \bar{s}_\nu^2 \bar{s}_\rho^2 \bar{s}_\sigma^2 - d_4 \sum_{\nu\neq\mu} \bar{s}_\nu^4, \\ G_{\mu\nu}(k) &= \bar{s}_\mu \bar{s}_\nu \widetilde{G}_{\nu,\mu}(k), \end{aligned} \tag{9}$$

$$\widetilde{G}_{\nu,\mu}(k) = d_1 - d_2 \frac{(\bar{s}_\rho^2 + \bar{s}_\sigma^2)}{2} + d_3 \frac{\bar{s}_\rho^2 \bar{s}_\sigma^2}{3} + d_4 \bar{s}_\nu^2. \tag{10}$$

Here, the coefficients d_i distinguish the different choices of fat links

(1) Unimproved (naive):

$$d_1 = 0, \quad d_2 = 0, \quad d_3 = 0, \quad d_4 = 0. \tag{11}$$

(2) Fat7 links:

$$d_1 = 1, \quad d_2 = 1, \quad d_3 = 1, \quad d_4 = 0. \tag{12}$$

(3) HYP (I) links:

$$\begin{aligned} &d_1 = (2/3)\alpha_1(1 + \alpha_2(1 + \alpha_3)), \\ &d_2 = (4/3)\alpha_1\alpha_2(1 + 2\alpha_3), \qquad d_3 = 8\alpha_1\alpha_2\alpha_3, \\ &d_4 = 0. \end{aligned} \tag{13}$$

We consider two choices for the α_i. The first was determined in [5] using a nonperturbative optimization procedure: $\alpha_1 = 0.75$, $\alpha_2 = 0.6$ $\alpha_3 = 0.3$ [we call this choice "HYP (I)"]. This gives

$$\begin{aligned} d_1 &= 0.89, \qquad d_2 = 0.96, \\ d_3 &= 1.08, \qquad d_4 = 0. \end{aligned} \tag{14}$$

(4) HYP (II) links: The second is chosen so as to remove $O(a^2)$ flavor-symmetry breaking couplings at tree-level. This choice, $\alpha_1 = 7/8$, $\alpha_2 = 4/7$, and $\alpha_3 = 1/4$ [we call this choice "HYP (II)"], gives

$$d_1 = 1, \quad d_2 = 1, \quad d_3 = 1, \quad d_4 = 0, \tag{15}$$

i.e., the same as for Fat7 links.

(5) Fat7+Lepage [$O(a^2)$ improved links]:

$$d_1 = 0, \quad d_2 = 1, \quad d_3 = 1, \quad d_4 = 1, \tag{16}$$

. For later convenience, we name the SU(3) projected Fat7 scheme "$\overline{\text{Fat7}}$".

In [8], we studied various fat links from the standpoint of renormalization to improve staggered fermions and it turns out that at the one-loop level, the renormalization of staggered fermion operators is identical between $\overline{\text{Fat7}}$ and HYP (II). In addition, it was explained that SU(3) projection plays a role in tadpole improvement for the staggered fermion doublers.

III. PENGUIN DIAGRAMS

Here, we study penguin diagrams in which one of the quarks in the four-fermion operator is contracted with one of the antiquarks to form a closed loop. The main goal is to calculate the penguin diagrams for improved staggered fermion operators and to provide a matching formula between the continuum and lattice operators at the one-loop level.

On the lattice, the gauge noninvariant four-fermion operators such as Landau gauge operators mix with lower dimension operators which are gauge noninvariant [14]. It

is required to subtract these contributions nonperturbatively. However, it is significantly harder to extract the divergent mixing coefficients in a completely nonperturbative way. This make it impractical to use gauge noninvariant operators for the numerical study of the CP violation. Hence, it is necessary to use gauge-invariant operators in order to avoid unwanted mixing with lower dimension operators. For this reason, we choose gauge-invariant operators in our numerical study.

In the staggered fermion formalism there are four penguin diagrams at the one-loop level as shown in Fig. 1. These diagrams of penguin type can mix with lower dimension operators in addition to four-fermion operators of the same dimension or higher. The mixing coefficients with lower dimension operators are proportional to inverse powers of the lattice spacing. The perturbation, however, is not reliable with divergent coefficients. Hence, we must use a nonperturbative method to determine them and subtract away the lower dimension operators. In the case of mixing with operators of the same dimension, the perturbative calculation is expected to be reliable as long as the size of the one-loop correction is small enough, which can be achieved naturally by improving the staggered operators using fat links.

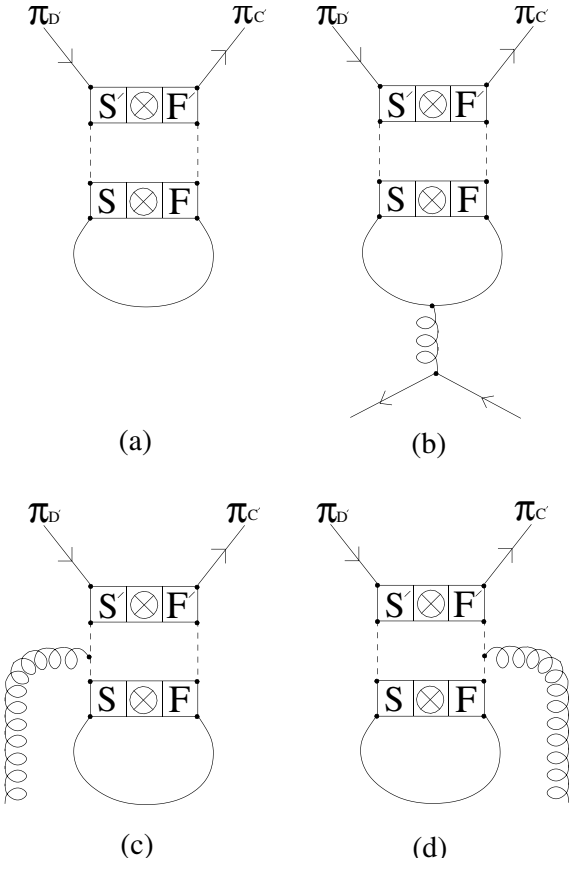

FIG. 1. Penguin diagrams for the staggered fermions.

In Fig. 1, diagrams (a) and (b) have their correspondence in the continuum and diagrams (c) and (d) do not have any continuum correspondence. However, diagrams (c) and (d) play an essential role in keeping the gauge invariance in the final sum. In other words, the gauge invariance is broken without them.

First, we overview the role of each diagram in the gauge invariance and present the details later. Basically, the contribution from diagrams (c) and (d) can be reexpressed as a sum of two separate terms: diagram (e) and (f) in Fig. 2. We observe that the sum of diagram (a) of Fig. 1 and diagram (e) of Fig. 2 produces bilinear operators in a gauge-invariant form as shown in Fig. 3. It turns out that the contribution from diagram (b) in Fig. 1 and diagram (f) in Fig. 2 leads to four-fermion operators of our interest in a gauge-invariant form, which are typically called ''Penguin diagrams'' in the literature as shown in Fig. 4. Once more, we emphasize that diagrams (c) and (d) [or equivalently (e) and (f)] are essential to keep the gauge invariance.

A. Penguin operators on the lattice

In order to construct a lattice version of continuum penguin operators, we need some guidelines, because the staggered fermions carry four degenerate tastes by construction, unlike the continuum fermions. Hence, a closed loop of staggered quarks contains four degenerate tastes running around it, rather than a single quark, which needs to be normalized properly by $1/N_f = 1/4$. Penguin dia-

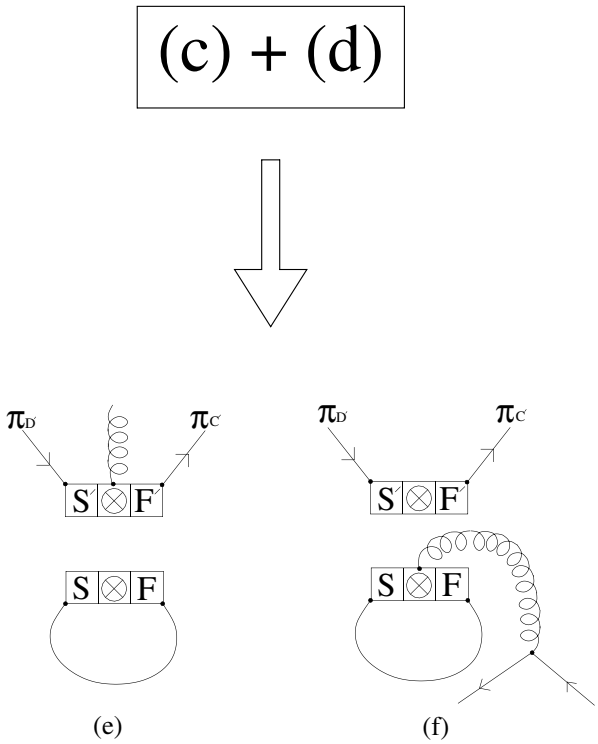

FIG. 2. Diagram identity: $(c) + (d) = (e) + (f)$.

grams occur for operators which belongs to octet irrep of the continuum flavor SU(3) symmetry. Apart from the overall factor, the calculation is identical for all the penguin operators of our interest [14,31]. Therefore, we may choose the following operator as a representative without loss of generality:

$$\mathcal{O}^{\mathrm{Cont}}_{S',S} \quad \longleftrightarrow \quad \mathcal{O}^{\mathrm{Latt}}_{S'F',SF}, \tag{17}$$

where the operators are defined as

$$\mathcal{O}^{\mathrm{Cont}}_{S',S} = [\bar{\psi}_s \gamma_{S'} \psi_d][\bar{\psi}_u \gamma_S \psi_u],$$
$$\mathcal{O}^{\mathrm{Latt}}_{S'F',SF} = \frac{1}{N_f^2}[\bar{\chi}_s \overline{(\gamma_{S'} \otimes \xi_{F'})} \chi_d][\bar{\chi}_u \overline{(\gamma_S \otimes \xi_F)} \chi_u].$$

Here, we adopt the two spin trace formalism [21], color contractions with gauge links are dropped for brevity, and the subscripts *s, d, u* represent the continuum quark flavors. Here we select the continuum flavors so that there is only one possibility of up quark contraction to form a closed loop, leading to a penguin diagram. The bilinear with strange and down quarks behaves as a spectator in the calculation. This choice of continuum flavor assignment was suggested originally in [14].

Penguin diagrams of the above operators lead to mixing with the same class of SU(3) octet operators (penguin operators):

$$\mathcal{O}^{\mathrm{Cont,P}}_{S',S} = [\bar{\psi}_s \gamma_{S'} \psi_d] \sum_q [\bar{\psi}_q \gamma_S \psi_q], \tag{18}$$

$$\mathcal{O}^{\mathrm{Latt,P}}_{S'F',SF} = \frac{1}{N_f^2}[\bar{\chi}_s \overline{(\gamma_{S'} \otimes \xi_{F'})} \chi_d] \sum_q [\bar{\chi}_q \overline{(\gamma_S \otimes \xi_F)} \chi_q], \tag{19}$$

where the sums run over the active light flavors such as *u, d, s*.

We adopt the same notation as in [14,24] to incorporate two different color contractions:

$$\vec{\mathcal{O}} = \begin{pmatrix} \mathcal{O}_I \\ \mathcal{O}_{II} \end{pmatrix}. \tag{20}$$

The contribution from the color two trace operator, $\mathcal{O}_{II}$ vanishes in the penguin diagram because it is proportional to $\mathrm{Tr}(T^a) = 0$ [T^a is the SU(3) group generator which is traceless]. Hence, it is sufficient to work only on the color one trace operator, $\mathcal{O}_I$. This simplifies the matching formula.

$$(\mathcal{O}_i^{\mathrm{Cont}})_I = (\mathcal{O}_i^{\mathrm{Latt}})_I + \frac{g^2}{(4\pi)^2} \sum_j Z_{ij} (\vec{P} \cdot \vec{\mathcal{O}}_j^{\mathrm{Latt}}), \tag{21}$$

where *i, j* includes both the spin and taste indices, and the projection vector is

$$\vec{P} = \left(+\frac{1}{2}, -\frac{1}{6} \right). \tag{22}$$

The Z_{ij} have two separate contributions: one from the continuum operators and the other from the lattice operators

$$Z_{ij} = Z_{ij}^{\mathrm{Cont}} - Z_{ij}^{\mathrm{Latt}}. \tag{23}$$

The main goal of this paper is to calculate Z_{ij}^{Latt}, since Z_{ij}^{Cont} is well known [32].

B. Feynman diagrams

Using the Feynman rules described in Sec. II, we express the analytical form of the Feynman diagrams presented in Fig. 1. Diagram (a) of Fig. 1 contains only mixing with bilinears and combined with diagram (e) of Fig. 2 makes the bilinears gauge invariant as shown in Fig. 3.

$$G_{(a)} = -\frac{1}{N_f} H_\mu^{I(a)}, \tag{24}$$

$$H_\mu^{I(a)} = \delta_{cd} \overline{\overline{(\gamma_{S'} \otimes \xi_{F'})}}_{C'D'} \frac{1}{16} \sum_{AB} \overline{(\gamma_S \otimes \xi_F)}_{AB} \cdot I_{AB}^{(a)}, \tag{25}$$

$$I_{AB}^{(a)} = \int_p \exp(ip \cdot (A - B))[S_F(p)]_{BA}. \tag{26}$$

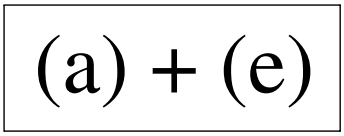

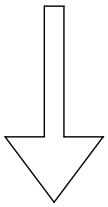

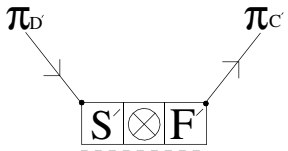

(g)

FIG. 3. Bilinear mixing.

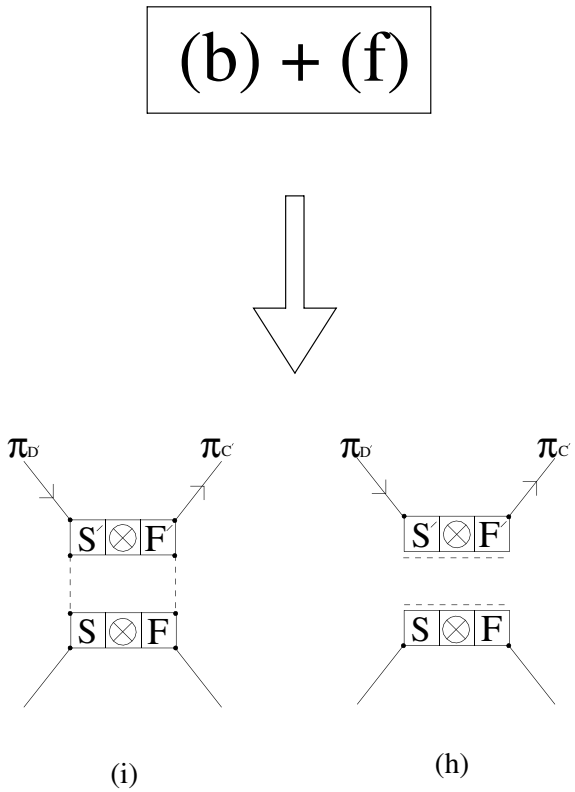

FIG. 4. Mixing with penguin operators.

Diagram (b) of Fig. 1, combined with diagram (f), leads to mixing with four-fermion operators as shown in Fig. 4. Using the Feynman rules described in Sec. II we can express the diagram (b) as follows:

$$G_{(b)} = -\frac{1}{N_f}\int_k H_\mu^{I,(b)}(k)\cdot D_{\mu\nu}^{IJ}(k) \cdot V_\nu^J(p+\pi_C, -q-\pi_D, -k), \tag{27}$$

$$H_\mu^{I,(b)}(k) = (-ig)T_{cd}^I \overline{\overline{(\gamma_{S'}\otimes\xi_{F'})}}_{C'D'} \frac{1}{16}\sum_{AB}\overline{(\gamma_S\otimes\xi_F)}_{AB} \times \exp\left[i\frac{k}{2}\cdot(A+B)\right]\cdot I_{AB}^{(b)}(k), \tag{28}$$

$$I_{AB}^{(b)}(k) = \int_p \exp(ip\cdot(A-B))\left\{\left[S_F\left(p-\frac{k}{2}\right)\right] \cdot\cos(p_\mu)\overline{(\gamma_\mu\otimes 1)}\cdot\left[S_F\left(p+\frac{k}{2}\right)\right]\right\}_{BA}. \tag{29}$$

Diagrams (c) and (d) of Fig. 1 contain mixing with bilinears and four-fermion operators as shown in Fig. 2. These two diagrams play an essential role in keeping the gauge invariance of the final results.

$$G_{(c)} = -\frac{1}{N_f}H_\mu^{I,(c)}(k), \tag{30}$$

$$H_\mu^{I,(c)}(k) = (+ig)T_{cd}^I\frac{1}{16}\sum_{A,B}\overline{(\gamma_S\otimes\xi_F)}_{AB} \times\frac{1}{16}\sum_{A',B'}(-1)^{C\cdot A'}\overline{(\gamma_{S'}\otimes\xi_{F'})}_{A'B'}(-1)^{D\cdot B'} \times(B-A')_\mu f_{A'B}^\mu(k)I_{AB}^{(a)}, \tag{31}$$

$$G_{(d)} = -\frac{1}{N_f}H_\mu^{I,(d)}(k), \tag{32}$$

$$H_\mu^{I,(d)}(k) = (+ig)T_{cd}^I\frac{1}{16}\sum_{A,B}\overline{(\gamma_S\otimes\xi_F)}_{AB} \times\frac{1}{16}\sum_{A',B'}(-1)^{C\cdot A'}\overline{(\gamma_{S'}\otimes\xi_{F'})}_{A'B'} \times(-1)^{D\cdot B'}(B'-A)_\mu f_{AB'}^\mu(k)I_{AB}^{(a)}. \tag{33}$$

C. Gauge invariance

As shown in Fig. 2, diagrams (c) and (d) of Fig. 1 can be expressed as a sum of diagrams (e) and (f). As a consequence of this, diagrams (b) and (f) lead to a gauge-invariant form of penguin operator and diagrams (a) and (e) lead to a gauge-invariant bilinear operator.

First, let us derive the relationship shown in Fig. 2. We begin with a simple identity for diagram (b):

$$\sum_\mu 2\sin\left(\frac{k_\mu}{2}\right)\cdot H_\mu^{I,(b)}(k) = (ig)T_{cd}^I\overline{\overline{(\gamma_{S'}\otimes\xi_{F'})}}_{C'D'} \cdot\frac{1}{16}\sum_{AB}\overline{(\gamma_S\otimes\xi_F)}_{AB} \cdot[\exp(ik\cdot A)-\exp(ik\cdot B)]\cdot I_{AB}^{(a)}. \tag{34}$$

The continuum correspondence of the above Eq. (34) vanishes but the right-hand side (rhs) of Eq. (34) is not zero. Then, what is going on with the gauge invariance? It turns out that there exists an additional term which cancels out this term, which is the focal point of this section.

The same kind of identities for diagrams (c) and (d) can be expressed in terms of diagrams (e) and (f).

$$\sum_\mu 2\sin\left(\frac{k_\mu}{2}\right)\cdot\left(H_\mu^{I,(c)}(k)+H_\mu^{I,(d)}(k)\right) = \sum_\mu 2\sin\left(\frac{k_\mu}{2}\right)\cdot\left(H_\mu^{I,(e)}(k)+H_\mu^{I,(f)}(k)\right). \tag{35}$$

Here, the $H_\mu^{I,(e)}(k)$ and $H_\mu^{I,(f)}(k)$ are defined as

$$H_\mu^{I,(e)}(k) = (+ig)T^I_{cd}\frac{1}{16}\sum_{A',B'}(-1)^{C'\cdot A'}\overline{(\gamma_{S'}\otimes\xi_{F'})}_{A'B'} \cdot(-1)^{D'\cdot B'}(B'-A')_\mu f^\mu_{A'B'}(k) \cdot\frac{1}{16}\sum_{A,B}\overline{(\gamma_S\otimes\xi_F)}_{AB}I^{(a)}_{AB}, \tag{36}$$

$$H_\mu^{I,(f)}(k) = (+ig)T^I_{cd}\overline{\overline{(\gamma_{S'}\otimes\xi_{F'})}}_{C'D'} \cdot\frac{1}{16}\sum_{A,B}\overline{(\gamma_S\otimes\xi_F)}_{AB}(B-A)_\mu f^\mu_{AB}(k)\cdot I^{(a)}_{AB}. \tag{37}$$

A derivation of the identity given in Eq. (35) is given in Appendix A.

Note that $H_\mu^{I,(e)}(k)$ can be factorized into two bilinears: one bilinear has a single gluon emitted and the other bilinear forms a closed fermion loop identical to that of diagram (a). Unlike the continuum operators, the staggered operators are nonlocal and gauge links must be inserted between the quark and antiquark fields to make them gauge invariant. Thus, at $\mathcal{O}(g)$, we must have $H_\mu^{I,(e)}(k)$ to keep the gauge invariance of the spectator bilinear. Of course, this is completely a lattice artifact, which will vanish in the limit of zero lattice spacing, $a = 0$. Let us explain this bilinear mixing in detail in the next subsection.

D. Bilinear mixing

Here, we combine diagrams (a) and (e) and show that they form a gauge-invariant bilinear.

$$H_\mu^{I,(a)} + H_\mu^{I,(e)}(k) = \frac{1}{16}\sum_{A',B'}(-1)^{C'\cdot A'}\overline{(\gamma_{S'}\otimes\xi_{F'})}_{A'B'}(-1)^{D'\cdot B'} \cdot[\delta_{cd} + (iga)T^I_{cd}(B'-A')_\mu f^\mu_{A'B'}(k)] \cdot\frac{1}{16}\sum_{A,B}\overline{(\gamma_S\otimes\xi_F)}_{AB}I^{(a)}_{AB}. \tag{38}$$

Here, the term enclosed in square brackets is nothing but an expansion of gauge link $\mathcal{V}(y_A, y_B)$ in powers of the gauge coupling g. Note that the closed loop part behaves as a constant defined as

$$X_{(a+e)} = \frac{1}{16}\sum_{A,B}\overline{(\gamma_S\otimes\xi_F)}_{AB}I^{(a)}_{AB}. \tag{39}$$

Hence, the combined result of diagrams (a) and (e) becomes

$$H_\mu^{I,(a)} + H_\mu^{I,(e)}(k) \longrightarrow \frac{X_{(a+e)}}{a^3}[\bar\chi(y_A)\overline{(\gamma_{S'}\otimes\xi_{F'})}_{AB} \times \mathcal{V}(y_A, y_B)\chi(y_B)]. \tag{40}$$

Naturally, the next question would be what are the possible spins and flavors for $(\gamma_S\otimes\xi_F)$ in the closed loop. Since we are talking about the vacuum diagram, it must have the vacuum quantum number. Hence, the natural choice would be that $(\gamma_S\otimes\xi_F) = (1\otimes 1)$.

Another question would be how reliable is the coefficient $X_{(a+e)}$. Since we are talking about the divergent coefficient, hence, the perturbative determination of $X_{(a+e)}$ is highly unreliable because the contribution from the truncated terms are also divergent as we approach to zero lattice spacing. Hence, this coefficient must be determined using a nonperturbative method.

E. Penguin operator mixing

Here, we want to present the main results of Penguin diagrams: mixing with penguin operators at the one-loop level. First, we address the issue of the gauge invariance. Basically, we want to show how the rhs of Eq. (34) cancels out. From the definition of $H_\mu^{I,(f)}(k)$ given in Eq. (37) it is easy to show the following Ward identity:

$$\sum_\mu 2\sin\left(\frac{k_\mu}{2}\right)\cdot(H_\mu^{I,(b)}(k) + H_\mu^{I,(f)}(k)) = 0. \tag{41}$$

This illustrates that, unlike the continuum, we need diagram (f) to keep the gauge invariance of diagram (b), which is a pure lattice artifact originating from using staggered fermions when constructing operators on the lattice.

Now, we turn to explicit calculation of the mixing with penguin operators. First, we define $I^{(c)}_{AB}$ in terms of $I^{(a)}_{AB}$ in Eq. (26) as follows:

$$I^{(c)}_{AB} \equiv (B-A)_\mu\cdot I^{(a)}_{AB} = \int_p \exp(ip\cdot(A-B))\cdot\{[S_F(p)] \cdot\cos(p_\mu)\overline{(\gamma_\mu\otimes 1)}[S_F(p)]\}_{BA}. \tag{42}$$

Using $I^{(c)}_{AB}$, we can collect diagrams (b) and (f) into such a form that all of the nice features necessary for the gauge invariance and the infrared behavior are visible at a glance.

$$H_\mu^{I,(b+f)}(k) \equiv H_\mu^{I,(b)}(k) + H_\mu^{I,(f)}(k) = (-ig)T^I_{cd}\overline{\overline{(\gamma_{S'}\otimes\xi_{F'})}}_{C'D'}\frac{1}{16}\sum_{AB} \cdot\overline{(\gamma_S\otimes\xi_F)}_{AB}\exp\left[i\frac{k}{2}\cdot(A+B)\right] \cdot[I^{(b)}_{AB}(k) - I^{(c)}_{AB}]. \tag{43}$$

This result is identical to that originally presented in [14].

Regarding the infrared behavior, note that

$$\lim_{k\to 0} I^{(b)}_{AB}(k) = I^{(c)}_{AB}.$$

Hence, this confirms that $H_\mu^{I,(b+f)}(k)$ vanishes when $k = 0$. In addition, the quark mass behaves as an infrared regulator such that the integrals of $I^{(b)}_{AB}(k)$ and $I^{(c)}_{AB}$ are infrared safe.

As shown in Eq. (41), $H_\mu^{I,(b+f)}(k)$ also satisfies the Ward identity coming from gauge invariance:

$$\sum_\mu \sin\left(\frac{k_\mu}{2}\right)\cdot H_\mu^{I,(b+f)}(k)=0 \tag{44}$$

for all values of k.

Now we turn to explicit calculation of $H_\mu^{I,(b+f)}(k)$ in such a form as we can use for matching to the continuum. The mixing contributions comes not only from $k\sim 0$ but also, in principle, from $k\sim \pi/a\cdot A$ for any arbitrary hypercubic vector A. Here, we first consider $k\sim 0$ as in the continuum.

$$H_\mu^{I,(b+f)}(k)=(-ig)T^I_{cd}\overline{\overline{(\gamma_{S'}\otimes\xi_{F'})}}_{CD}\cdot\frac{1}{16}\sum_{A,B}\overline{(\gamma_S\otimes\xi_F)}_{AB}[P_\mu(k)]_{BA}, \tag{45}$$

$$\begin{aligned}[P_\mu(k)]_{BA}=&-\frac{i}{(4\pi)^2}\sum_{\alpha,\nu,\rho}\epsilon_{\mu\alpha\nu\rho}k_\alpha\overline{(\sigma_{\nu\rho}\otimes\xi_{\nu 5})}_{BA}\cdot I_a\\&+\frac{im}{(4\pi)^2}\sum_\alpha k_\alpha\overline{(\sigma_{\mu\alpha}\otimes 1)}_{BA}\cdot I_b\\&+\frac{i^2}{(4\pi)^2}\sum_\alpha(\delta_{\mu\alpha}k^2-k_\mu k_\alpha)\overline{(\gamma_\alpha\otimes 1)}_{BA}\cdot I_c,\end{aligned} \tag{46}$$

where the lattice-regularized finite integrals I_a, I_b and I_c are given in Appendix B. Note that this result for the improved staggered fermions is identical to that for the unimproved staggered fermions presented in [14]. This equivalence will be discussed in detail later when we present Theorem 1.

The first term in Eq. (46) describes mixing of the four-fermion operator with a bilinear with gluon emission:

$$\begin{aligned}&[\bar\chi_s\overline{(\gamma_{S'}\otimes\xi_{F'})}\chi_d][\bar\chi_u\overline{(\sigma_{\nu\rho}\otimes\xi_{\nu 5})}\chi_u]\\&\longrightarrow[\bar\chi_s\overline{(\gamma_{S'}\otimes\xi_{F'})}\widetilde{F}_{\nu\rho}\chi_d].\end{aligned} \tag{47}$$

This corresponds to mixing with a dimension 5 operator. From the standpoint of physics, this mixing belongs to a class of unphysical operators because none of the operators of our interest possesses a flavor structure of $\xi_{\nu 5}$.

Similarly, the second term in Eq. (46) corresponds to mixing of the four-fermion operators with a bilinear:

$$\begin{aligned}&[\bar\chi_s\overline{(\gamma_{S'}\otimes\xi_{F'})}\chi_d][\bar\chi_u\overline{(\sigma_{\mu\alpha}\otimes 1)}\chi_u]\\&\longrightarrow m[\bar\chi_s\overline{(\gamma_{S'}\otimes\xi_{F'})}F_{\mu\alpha}\chi_d].\end{aligned} \tag{48}$$

This represents mixing with a dimension 6 bilinear which has its correspondence in the continuum. However, this operator vanishes in the chiral limit and so it corresponds to a higher order in the chiral perturbation. In addition, the spin structure of the tensor does not appear in the original set of operators of our interest and so this mixing can occur, if any, at order g^4. Hence, by convention, this term is dropped from the analysis [14,31].

It is the third term in Eq. (46) that corresponds to mixing with penguin operators. To complete the operator construction, the gluon needs to be connected to the external fermion line as follows.

$$\begin{aligned}G_{(b+f)}=&-\frac{1}{N_f}\int_k H_\mu^{I,(b+f)}(k)\cdot D^{IJ}_{\mu\nu}(k)\\&\cdot V^J_\nu(p+\pi_C,-q-\pi_D,-k),\end{aligned} \tag{49}$$

where V^J_ν corresponds to the fermion vertex emitting one gluon in [21]. Here, $D^{IJ}_{\mu\nu}(k)$ represents the gluon propagator of the thin or fat links which can be collectively written in terms of $\hat k_\mu=2\sin(k_\mu/2)$ as

$$D^{IJ}_{\mu\nu}(k)=\delta_{IJ}\sum_{\alpha,\beta}h_{\mu\alpha}(k)h_{\nu\beta}(k)\left[\frac{\delta_{\alpha\beta}}{\hat k^2}-(1-\lambda)\cdot\frac{\hat k_\alpha\hat k_\beta}{[\hat k^2]^2}\right] \tag{50}$$

in a general covariant gauge, where $\hat k^2=\sum_\beta\hat k_\beta^2$. It turns out that only the diagonal part of $h_{\mu\alpha}(k)$ contributes mainly because the off-diagonal term of $h_{\mu\alpha}(k)$ is proportional to $\hat k_\mu\hat k_\alpha\to k_\mu k_\alpha$ and so the contribution from the off-diagonal term of $h_{\mu\alpha}(k)$ vanishes due to a simple identity: $(\delta_{\mu\alpha}k^2-k_\mu k_\alpha)\cdot k_\mu=0$.

$$(\delta_{\mu\nu}k^2-k_\mu k_\nu)h_{\mu\alpha}(k)=(\delta_{\mu\nu}k^2-k_\mu k_\nu)\delta_{\mu\alpha}h_{\mu\mu}(k). \tag{51}$$

In addition, since $h_{\mu\mu}(k)=1+\mathcal{O}(a^2k^2)$, the same identity also guarantees that the gauge fixing term proportional to $(1-\lambda)$ also vanishes for the leading term in the limit of $k\to 0$, which insures gauge invariance. In summary, we can claim that in the low momentum limit of $k\to 0$,

$$\begin{aligned}(\delta_{\mu\alpha}k^2-k_\mu k_\alpha)\cdot D^{IJ}_{\mu\nu}(k)=&\,\delta_{IJ}\delta_{\mu\nu}[h_{\mu\mu}(k)]^2\frac{1}{k^2}\\&\cdot(\delta_{\mu\alpha}k^2-k_\mu k_\alpha).\end{aligned} \tag{52}$$

Another important ingredient is that the $k_\mu k_\alpha$ part of $(\delta_{\mu\alpha}k^2-k_\mu k_\alpha)$ cannot contribute in the on-shell limit. Using the equations of motion for the staggered fermions, we can prove that regardless of quark mass,

$$\sum_\mu\sin\left(\frac{k_\nu}{2}\right)\cdot V^J_\nu(p,-q,-k)=0. \tag{53}$$

Hence, in the limit of small momentum, the $\delta_{\mu\nu}k_\mu k_\alpha$ term vanishes by the equations of motion. In addition, in the low momentum limit,

$$\exp\left[i\frac{ka}{2}\cdot(A+B)\right]=1+\mathcal{O}(ka) \tag{54}$$

and we are interested only in the leading term, since the contribution from the remaining higher dimension opera-

tors is supposed to vanish as we approach to the continuum ($a = 0$).

Now we can simplify $G_{(b+f)}$ defined in Eq. (49) at small k,

$$G_{(b+f)} = \left(-\frac{1}{N_f}\right)\frac{g^2}{(4\pi)^2}\left(\sum_I T^I_{cd}T^I_{ab}\right)I_c \cdot \sum_\mu \overline{\overline{(\gamma_{S'} \otimes \xi_{F'})}}_{C'D'} \overline{\overline{(\gamma_\mu \otimes 1)}}_{CD} \cdot \delta_{S,\mu}\delta_{F,1}[h_{\mu\mu}(k)]^2, \quad (55)$$

where $k = q - p$ is strictly on shell. From the above Eq. (55), we can derive an interesting theorem:

Theorem 1 (Equivalence).—At the one-loop level, the diagonal mixing coefficients of penguin diagrams are identical between (a) the unimproved (naive) staggered operators constructed using the thin links and (b) the improved staggered operators constructed using the fat links such as HYP (I), HYP (II), Fat7, Fat7+Lepage, and $\overline{\text{Fat7}}$ [33].

Proof 1.1.—In the case of the unimproved staggered operators, $h_{\mu\mu}(k) = 1$ by definition. The improvement using the fat links such as HYP, Fat7, Lepage + Fat7, $\overline{\text{Fat7}}$, in general, leads to $h_{\mu\mu}(k)$ as defined in Eq. (11). The role of the additional terms proportional to d_i is to suppress the high momentum gluon interactions at the cutoff scale (π/a). Hence, by construction, these additional terms cannot change the dispersion in the low momentum region. In other words, in the limit of $k \to 0$,

$$h_{\mu\mu}(k) = 1 + \mathcal{O}(k^2a^2). \quad (56)$$

Here, the $\mathcal{O}(k^2a^2)$ term corresponds to higher dimension operators, whose contribution vanishes in the limit of $a = 0$. Hence, this term is irrelevant to the penguin mixing of our interest. It is only the leading term of Eq. (56) that contributes to the mixing with penguin operators. The $[h_{\mu\mu}(k)]^2$ term is, if any, the only possible source of difference introduced by the improvement. However, the contribution from $[h_{\mu\mu}(k)]^2$ is, by construction, identical in the low momentum limit before and after the improvement. Therefore, this leads us to the conclusion that the mixing coefficients with penguin operators must be identical for the staggered operators constructed using both thin links and fat links such as HYP, Fat7, Lepage + Fat7, and $\overline{\text{Fat7}}$. This completes the proof of the theorem.

As a consequence of Theorem 1, it is trivial to obtain the diagonal mixing coefficients from Eq. (55).

$$Z^{\text{Latt}}_{ii} = -\frac{1}{N_f}I_c, \quad (57)$$

where i represents $(\gamma_\mu \otimes 1)$. This is our final result.

F. High momentum gluons and off-diagonal mixing.

By construction, gluons carrying a momentum close to $k \sim \pi/a$ are physical in staggered fermions and lead to taste-changing interactions, which is a pure lattice artifact. Let us consider a vertex where a gluon carries a momentum $k + \Pi_C$ where $\Pi_C \equiv \pi/a \cdot C$ and a quark/antiquark has momentum $(p + \Pi_A)/(q + \Pi_B)$, respectively. Here we assume that $|k|, |p|, |q| \ll \pi/a$. This vertex can be expressed as follows:

$$h_{\mu\nu}(k + \Pi_C) \cdot V^J_\nu(p + \Pi_A, -q - \Pi_B, k + \Pi_C) = (-ig)T^J\bar{\delta}(p - q + k)\overline{\overline{(\gamma_{\nu\tilde{C}} \otimes \xi_{\tilde{C}})}}_{A,B} \cdot \left[\frac{1 + (-1)^{C_\nu}}{2} + \mathcal{O}(ka)\right]h_{\mu\nu}(k + \Pi_C). \quad (58)$$

Here, obviously we need to choose $C_\nu = 0$. In other words, the longitudinal mode is not allowed to carry high momentum in the gluon vertex mainly because this is unphysical and violates helicity conservation. In the case of unimproved (naive) staggered fermions, $h_{\mu\nu}(k + \Pi_C) = \delta_{\mu\nu}$ regardless of Π_C. Hence, it is permissible to mix with the taste $\xi_{\tilde{C}}$ (we call this off-diagonal mixing below) and the mixing coefficient is substantial [14]. In contrast, in the case of the improved staggered fermions using the fat links of our interest such as Fat7, $\overline{\text{Fat7}}$ and HYP (II),

$$h_{\mu\nu}(k + \Pi_C) = 0 + \mathcal{O}(k^2a^2) \quad (59)$$

when $C_{\rho\neq\nu} = 1$ in at least one transverse direction. The vertex also vanishes when $C_\nu = 1$. Hence, this off-diagonal mixing is absent at the one-loop level. Since we adopt either $\overline{\text{Fat7}}$ or HYP (II) as our improvement scheme in our numerical study, we rejoice in this absence of unphysical off-diagonal mixing when we analyze the data.

In the case of the improvement using HYP (I) and Fat7 + Lepage, $h_{\mu\nu}(k + \Pi_C)$ does not vanish exactly but it is significantly suppressed. Correspondingly, the off-diagonal mixing is similarly suppressed.

G. Tadpole improvement

In [24], the procedure of tadpole improvement for the staggered four−fermion operators is presented. The tadpole improvement factor is given, basically, in powers of u_0. In perturbation, the contribution from this is of order g^2 so that only the tadpole improvement of the original operator at the tree-level can contribute at the g^2 order. Hence, the one-loop result for penguin operators are of order g^2 and the tadpole improvement can change the result only at the order of g^4. In other words, the tadpole improvement corrections included when we calculate the current-current diagrams are complete at g^2 order and so there is no additional correction from the tadpole improvement to the penguin diagrams. This argument holds valid not only for the diagonal mixing but also for the off-diagonal mixing.

IV. CONCLUSION

We have studied penguin diagrams for various improved staggered fermions at the one-loop level. The diagonal mixing occurs only when the original operator has the spin and taste structure of $(\gamma_\mu \otimes 1)$ regardless of that of the spectator bilinear. The main result summarized in Theorem 1 is that the diagonal mixing coefficient is identical between the unimproved staggered operators and the improved staggered operators constructed using fat links such as Fat7, Fat7 + Lepage, $\overline{\text{Fat7}}$, HYP (I) and HYP (II). This is a direct consequence of the fact that the contribution from the improvement changes only the mixing with higher dimension operators and off-diagonal operators, which are unphysical. However, Theorem 1 has such a limitation that it does not apply directly to the case of the AsqTad staggered formulation, in which case there is an ambiguity of choosing the fat links for the operators. In addition, the mixing with off-diagonal operators vanishes for Fat7, $\overline{\text{Fat7}}$ and HYP (II). In the case of Fat7 + Lepage and HYP (I), the off-diagonal mixing is significantly suppressed by the factor of $[h_{\mu\mu}]^2$.

The results of this paper, combined with those of the current-current diagrams in [6], provide a complete set of matching for ϵ'/ϵ with all corrections of $\mathcal{O}(g^2)$ included. In our numerical study of the CP violation, we adopt $\overline{\text{Fat7}}$ and HYP (II). It turns out that this choice has one additional advantage of the absence of off-diagonal mixing in penguin diagrams as well as those advantages presented in [6–8].

ACKNOWLEDGMENTS

We would like to express our sincere gratitude to S. Sharpe for his consistent encouragement and helpful discussion on this paper. We would like to thank T. Bhattacharya, N. Christ, G. Fleming, R. Gupta, G. Kilcup and R. Mawhinney for their support on the staggered ϵ'/ϵ project. This work was supported in part by the BK21 program at Seoul National University, by an Interdiciplinary Research Grant of Seoul National University and by KOSEF through Grant No. R01-2003-000-10229-0.

APPENDIX A: DERIVATION OF EQ. (35)

First, we define the common factor Y as

$$Y = (ig)T^I_{cd}\frac{1}{16}\sum_{A'B'}(-1)^{C'\cdot A'}\overline{(\gamma_{S'}\otimes\xi_{F'})}_{A'B'}(-1)^{D'\cdot B'} \times \frac{1}{16}\sum_{AB}\overline{(\gamma_S\otimes\xi_F)}_{AB}I^{(a)}_{AB}. \quad \text{(A1)}$$

Using this notation, we can simplify the identities as follows.

$$\sum_\mu 2\sin\left(\frac{k_\mu}{2}\right)\cdot H^{I,(c)}_\mu(k) = Y\cdot[e^{ik\cdot B} - e^{ik\cdot A'}], \quad \text{(A2)}$$

$$\sum_\mu 2\sin\left(\frac{k_\mu}{2}\right)\cdot H^{I,(d)}_\mu(k) = Y\cdot[e^{ik\cdot B'} - e^{ik\cdot A}], \quad \text{(A3)}$$

$$\sum_\mu 2\sin\left(\frac{k_\mu}{2}\right)\cdot H^{I,(e)}_\mu(k) = Y\cdot[e^{ik\cdot B'} - e^{ik\cdot A'}], \quad \text{(A4)}$$

$$\sum_\mu 2\sin\left(\frac{k_\mu}{2}\right)\cdot H^{I,(f)}_\mu(k) = Y\cdot[e^{ik\cdot B} - e^{ik\cdot A}]. \quad \text{(A5)}$$

Using these identities, it is easy to derive Eq. (35).

APPENDIX B: FINITE INTEGRALS

We use the following abbreviation to represent the integration measure and its normalization factor.

$$\int_p \equiv (16\pi^2)\Pi_\mu\int_{-\pi}^{\pi}\frac{dp_\mu}{2\pi}. \quad \text{(B1)}$$

Using this notation, we can express I_a, I_b and I_c as follows.

$$I_a = \int_p F^2(p)\cos^2(p_\mu)\cos^2(p_\alpha)\sin^2(p_\nu) = +11.2293(3), \quad \text{(B2)}$$

$$I_b = \int_p F^2(p)\cos^2(p_\mu)\cos^2(p_\alpha) = 16[-\ln(4m^2a^2) - \gamma_E + F_{0000}] - 40.7773(6) + \mathcal{O}(m^2a^2), \quad \text{(B3)}$$

$$I_c = \int_p \frac{1}{6}F^2(p)[2 - \sin^2(p_\mu) - \sin^2(p_\alpha) - \sin^2(p_\mu)\sin^2(p_\alpha)] = \frac{16}{3}(-\ln(4m^2a^2) - \gamma_E + F_{0000}) - 9.5147(1) + \mathcal{O}(m^2a^2), \quad \text{(B4)}$$

where $\mu \neq \alpha \neq \nu$ and $F(p)$ is defined as

$$F(p) = \frac{1}{\sum_\mu \sin^2(p_\mu) + (ma)^2}. \quad \text{(B5)}$$

These integrals are also given in [14] and the results are consistent with each other.

[1] C. T. H. Davies *et al.*, Phys. Rev. Lett. **92**, 022001 (2004).
[2] J. F. Lagae and D. K. Sinclair, Phys. Rev. D **59**, 014511 (1999).
[3] P. Lepage, Phys. Rev. D **59**, 074502 (1999).
[4] K. Orginos and D. Toussaint, Phys. Rev. D **59**, 014501 (1999).
[5] A. Hasenfratz and F. Knechtli, Phys. Rev. D **64**, 034504 (2001).
[6] W. Lee and S. Sharpe, Phys. Rev. D **68**, 054510 (2003).
[7] W. Lee and S. Sharpe, Phys. Rev. D **66**, 114501 (2002).
[8] Weonjong Lee, Phys. Rev. D **66**, 114504 (2002).
[9] W. Lee *et al.*, hep-lat/0409047.
[10] M. Luscher and P. Weisz, Nucl. Phys. **B266**, 309 (1986).
[11] Howard Trottier, Nucl. Phys. (Proc. Suppl.) **B129**, 142 (1986).
[12] Quentin Mason, Ph.D. thesis, Cornell University, 2003.
[13] A. Buras *et al.*, Nucl. Phys. **B400**, 37 (1993).
[14] S. Sharpe and A. Patel, Nucl. Phys. **B417**, 307 (1994).
[15] K. Choi and W. Lee, Nucl. Phys. (Proc. Suppl.) **B129**, 438 (2004).
[16] M. F. L. Golterman and J. Smit, Nucl. Phys. **B245**, 61 (1984).
[17] K. Orginos *et al.*, Phys. Rev. D **60**, 054503 (1999).
[18] P. Lepage, Phys. Rev. D **59**, 074502 (1999).
[19] Maarten Golterman, Nucl. Phys. (Proc. Suppl.) **B73**, 906 (1999).
[20] H. Kluberg-stern *et al.*, Nucl. Phys. **B220**, 447 (1983).
[21] W. Lee and M. Klomfass, Phys. Rev. D **51**, 6426 (1995).
[22] S. Sharpe *et al.*, Nucl. Phys. **B286**, 253 (1987).
[23] S. Sharpe, Report No. DOE/ER/40614-5.
[24] Weonjong Lee, Phys. Rev. D **64**, 054505 (2001).
[25] A. Patel and S. Sharpe, Nucl. Phys. **B395**, 701 (1993).
[26] N. Ishizuka and Y. Shizawa, Phys. Rev. D **49**, 3519 (1994).
[27] D. Daniel and S. N. Sheard, Nucl. Phys. **B302**, 471 (1988).
[28] S. N. Sheard, Nucl. Phys. **B314**, 238 (1989).
[29] We heard that this is known and used in [25,30].
[30] C. Bernard and T. DeGrand, Nucl. Phys. (Proc. Suppl.) **B83**, 845 (2000).
[31] G. Buchalla *et al.*, Rev. Mod. Phys. **68**, 1125 (1996).
[32] C. Bernard, T. Draper, and A. Soni, Phys. Rev. D **36**, 3224 (1987).
[33] Note that AsqTad is *not* included in the list. In this case, by construction the operators are made of the fat links which are not the same as those used in the action due to the Naik term. In addition, the choice of the fat links is open and not unique.